Chapter 4
Properties of Probability Density Functions

The physical processes we study in this text are modeled using models including stochastic terms. Direct numerical simulations based on such stochastic models give results that are hard to interpret and it is therefore common to run many simulations and compute the average, and we have also seen that we can derive models governing the probability density functions. These are powerful tools that provide insight in the processes. In this chapter we will see that it is useful to have specific numbers that characterize stochastic variables and associated probability density functions. We encountered the equilibrium probability of being in the open or closed state (see, e.g., page 57) and we introduced probability density functions (see, e.g., page 30). Here we shall derive some specific (and common) characteristics of the probability density functions and discuss how these characteristics can be used to gain an understanding of calcium release. We will also show how the characteristics relate to the concepts already introduced and we will discuss how the characteristics vary as functions of the mutation severity index. Finally, we will show how the statistical characterizations can be used to evaluate the properties of theoretical drugs.

4.1 Probability Density Functions

Let us briefly recall the models under consideration. We consider the model

$$\bar{x}'(t) = \bar{\gamma}(t)v_r(c_1 - \bar{x}) + v_d(c_0 - \bar{x}) \tag{4.1}$$

of the calcium concentration of the dyad (see Fig. 2.1). Recall that v_r denotes the speed of release from the sarcoplasmic reticulum (SR) to the dyad, v_d denotes the speed of diffusion from the dyad to the cytosol, c_0 is the concentration of calcium

A. Tveito, G.T. Lines, *Computing Characterizations of Drugs for Ion Channels and Receptors Using Markov Models*, Lecture Notes in Computational Science and Engineering 111, DOI 10.1007/978-3-319-30030-6_4

ions in the cytosol, and c_1 is the calcium concentration in the SR; both c_0 and c_1 are assumed to be constant. The stochastic function $\bar{\gamma} = \bar{\gamma}(t)$ can be either zero (closed state) or one (open state) and the state is governed by the Markov model

$$C \underset{k_{co}}{\overset{k_{oc}}{\leftrightarrows}} O, \tag{4.2}$$

where k_{oc} and k_{co} are the rates associated with the Markov model. As discussed above, the probability density functions of the states of the Markov model are governed by the following system of partial differential equations:

$$\frac{\partial \rho_o}{\partial t} + \frac{\partial}{\partial x}(a_o \rho_o) = k_{co}\rho_c - k_{oc}\rho_o, \tag{4.3}$$

$$\frac{\partial \rho_c}{\partial t} + \frac{\partial}{\partial x}(a_c \rho_c) = k_{oc}\rho_o - k_{co}\rho_c, \tag{4.4}$$

where, as above, ρ_o and ρ_c are the probability density functions of the open and closed states, respectively. Furthermore, we recall that

$$a_o = v_r(c_1 - x) + v_d(c_0 - x), \tag{4.5}$$

$$a_c = v_d(c_0 - x). \tag{4.6}$$

The system of partial differential equations given by (4.3) and (4.4) is solved on the computational domain given by $\Omega = [c_0, c_+]$, where

$$c_+ = \frac{v_r c_1 + v_d c_0}{v_r + v_d},$$

and the boundary conditions are set up to ensure that there is no leak of probability across the boundaries (see page 37).

4.2 Statistical Characteristics

For the probability density functions given by the system (4.3) and (4.4), we can introduce the common statistical concepts of probability, expectation, and standard deviation. The probabilities of being in the open and closed states are given by

$$\pi_o = \int_\Omega \rho_o dx \text{ and } \pi_c = \int_\Omega \rho_c dx, \tag{4.7}$$

respectively. It is worth noting that these values are time dependent but independent of space (concentration). Furthermore, the sum of these probabilities adds up to one,

$$\pi_o(t) + \pi_c(t) = 1,$$

for all time. The expected values of the concentration are given by

$$E_o = \frac{1}{\pi_o}\int_\Omega x\rho_o dx \text{ and } E_c = \frac{1}{\pi_c}\int_\Omega x\rho_c dx \tag{4.8}$$

under the condition that the channels are open and closed, respectively. Finally, the standard deviations σ_o and σ_c are given by

$$\sigma_o^2 = \frac{1}{\pi_o}\int_\Omega x^2\rho_o dx - E_o^2, \tag{4.9}$$

$$\sigma_c^2 = \frac{1}{\pi_c}\int_\Omega x^2\rho_c dx - E_c^2. \tag{4.10}$$

We will show below how changes in the Markov model affect these characteristics and how the characteristics are influenced by the theoretical drugs. Generally, we have to solve the system (4.3) and (4.4) and then compute the statistical properties. However, we will see that in the special case in which the rate functions defining the Markov model, k_{oc} and k_{co}, are constant; we can compute some of the characteristics analytically. We will therefore start by considering such a case.

4.3 Constant Rate Functions

We consider the system (4.3) and (4.4) in the special case that both k_{oc} and k_{co} are constants (independent of the concentration x). If we integrate (4.3) and (4.4) over the interval Ω, we obtain the system

$$\pi_o' = k_{co}\pi_c - k_{oc}\pi_o, \tag{4.11}$$

$$\pi_c' = k_{oc}\pi_o - k_{co}\pi_c, \tag{4.12}$$

where we use the boundary conditions that state that there is no flux of probability across the boundaries.

4.3.1 Equilibrium Probabilities

When this system reaches equilibrium, the probabilities satisfy

$$k_{co}\pi_c = k_{oc}\pi_o \tag{4.13}$$

and since $\pi_o + \pi_c = 1$, we find that

$$\pi_o = \frac{k_{co}}{k_{oc} + k_{co}}, \tag{4.14}$$

$$\pi_c = \frac{k_{oc}}{k_{oc} + k_{co}}, \tag{4.15}$$

which we recognize as the probabilities o and c, respectively, derived directly from the equilibrium of the Markov model on page 57. This relation explains the connection between these two ways of considering the probability of being in a given state of the Markov model, but it is important to note that this relation only holds when the rate functions are constant.

4.3.2 Dynamics of the Probabilities

In the special case with only two states of the Markov model and constant rate functions, we can analytically compute how the probabilities evolve in time. If we use the fact that $\pi_o(t) + \pi_c(t) = 1$ for all time, we find that the system (4.11) and (4.12) can be reduced to one equation written in the form

$$\pi_o' = (k_{co} + k_{oc})\left(\frac{k_{co}}{k_{co} + k_{oc}} - \pi_o\right). \tag{4.16}$$

Suppose we know that the channel is closed at $t = 0$; then $\pi_o(0) = 0$ and we find the solution

$$\pi_o(t) = \frac{k_{co}}{k_{co} + k_{oc}}\left(1 - e^{-(k_{co}+k_{oc})t}\right). \tag{4.17}$$

We note that if the channel is closed at $t = 0$, the open probability reaches the equilibrium given by

$$\frac{k_{co}}{k_{co} + k_{oc}}$$

at an exponential rate in time and the exponent is given by $k_{co} + k_{oc}$ so that equilibrium is reached faster for higher rates.

4.3.3 Expected Concentrations

We still consider constant rate functions. In that case, we will show that the expected concentration in the case of open or closed channels can be obtained by solving a 2×2 linear system of ordinary differential equations. We start by considering the system defining the probability density functions,

$$\frac{\partial \rho_o}{\partial t} + \frac{\partial}{\partial x}(a_o \rho_o) = k_{co}\rho_c - k_{oc}\rho_o, \tag{4.18}$$

$$\frac{\partial \rho_c}{\partial t} + \frac{\partial}{\partial x}(a_c \rho_c) = k_{oc}\rho_o - k_{co}\rho_c. \tag{4.19}$$

Since

$$E_o \pi_o = \int_\Omega x \rho_o dx \text{ and } E_c \pi_c = \int_\Omega x \rho_c dx, \tag{4.20}$$

we find, using (4.18), that

$$(E_o \pi_o)_t = \int_\Omega x \frac{\partial \rho_o}{\partial t} dx \tag{4.21}$$

$$= -\int_\Omega x \frac{\partial}{\partial x}(a_o \rho_o)\, dx + k_{co}\int_\Omega x\rho_c dx - k_{oc}\int_\Omega x\rho_o dx \tag{4.22}$$

$$= -\int_\Omega x \frac{\partial}{\partial x}(a_o \rho_o)\, dx + k_{co}\pi_c E_c - k_{oc}\pi_o E_o. \tag{4.23}$$

Here the integral can be handled using integration by parts. The domain Ω is defined by the interval $[x_-, x_+] = [c_0, c_+]$ and we recall that $a_o\rho_o = a_c\rho_c = 0$ at $x = x_-$ and at $x = x_+$. Therefore, by using the definition of a_o given in (4.5), we obtain

$$-\int_{x_-}^{x_+} x \frac{\partial}{\partial x}(a_o \rho_o)\, dx = -\left[x\,(a_o\rho_o)\right]_{x_-}^{x_+} + \int_{x_-}^{x_+} a_o\rho_o dx \tag{4.24}$$

$$= (v_r c_1 + v_d c_0)\,\pi_o - (v_r + v_d)\,\pi_o E_o. \tag{4.25}$$

Consequently, we obtain

$$(E_o\pi_o)_t = (v_r c_1 + v_d c_0)\,\pi_o + k_{co}\pi_c E_c - (v_r + v_d + k_{oc})\,\pi_o E_o. \tag{4.26}$$

Similarly, we have

$$(E_c\pi_c)_t = \int_\Omega x\frac{\partial \rho_c}{\partial t}dx \tag{4.27}$$

$$= -\int_\Omega x\frac{\partial}{\partial x}\left(a_c\rho_c\right)dx + k_{oc}\int_\Omega x\rho_o dx - k_{co}\int_\Omega x\rho_c dx \tag{4.28}$$

$$= -\int_\Omega x\frac{\partial}{\partial x}\left(a_o\rho_o\right)dx + k_{oc}\pi_o E_o - k_{co}\pi_c E_c \tag{4.29}$$

and, by the definition (4.6) of a_c, we find that

$$-\int_{x_-}^{x_+}\frac{\partial}{\partial x}\left(a_c\rho_c\right)xdx = -\left[\left(a_c\rho_c\right)x\right]_{x_-}^{x_+} + \int_{x_-}^{x_+} a_c\rho_c dx \tag{4.30}$$

$$= v_d c_0\pi_c - v_d\pi_c E_c. \tag{4.31}$$

We therefore obtain

$$(E_c\pi_c)_t = v_d c_0\pi_c + k_{oc}\pi_o E_o - \left(v_d + k_{co}\right)\pi_c E_c. \tag{4.32}$$

Since we have already found explicit formulas for π_o and π_c, we can define

$$e_o = E_o\pi_o \text{ and } e_c = E_c\pi_c \tag{4.33}$$

and solve the system

$$e_o' = \left(v_r c_1 + v_d c_0\right)\pi_o + k_{co}e_c - \left(v_r + v_d + k_{oc}\right)e_o, \tag{4.34}$$

$$e_c' = v_d c_0\pi_c + k_{oc}e_o - \left(v_d + k_{co}\right)e_c. \tag{4.35}$$

When π_o, π_c, and e_o, e_c are computed, of course computing the expectations E_o and E_c is straightforward.

4.3.4 Numerical Experiments

In Figs. 4.1 and 4.2, we illustrate the properties derived above by presenting the results of numerical computations. The parameters used in the computations are given in Table 4.1. In Fig. 4.1, we show how the probability defined by (4.7) evolves as a function of time. The solid line is the exact solution given by the formula (4.17) and the crosses are based on the numerical solution of the system (4.3) and (4.4), where the probability defined by (4.7) is replaced by a Riemann sum based on the numerical solution. In Fig. 4.2, we show the evolution of the expected concentration for the open (solid) or closed (dashed) state, based on solving the system of

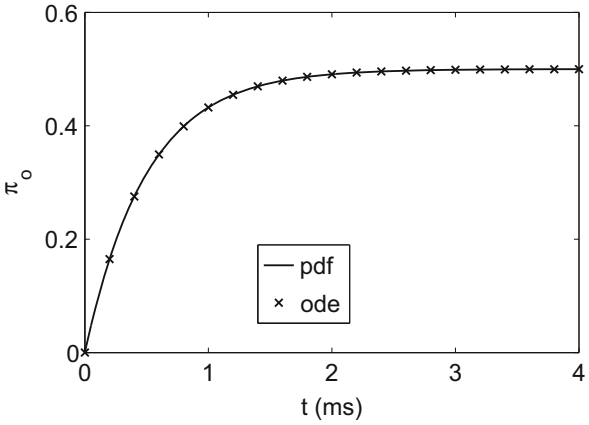

Fig. 4.1 Comparison of the theoretically derived open probability given by (4.17) with the numerical solution of the probability density functions defined by the system (4.3) and (4.4). In the latter case, the integrals (4.7) are replaced by Riemann sums

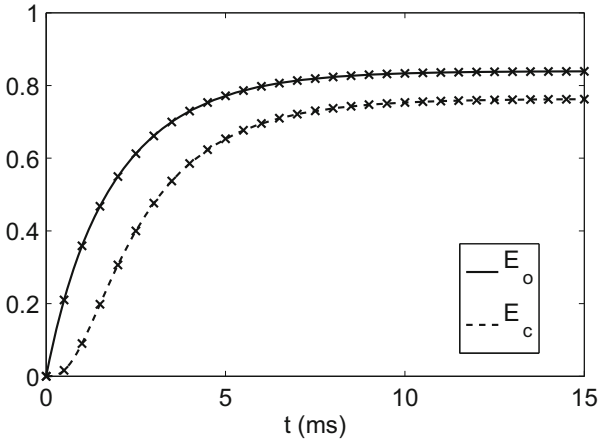

Fig. 4.2 Comparison of the theoretically derived expectations given by (4.33), where e_o and e_c are solutions of the system (4.34) and (4.35), with the numerical solution of the probability density functions defined by the system (4.3) and (4.4). In the latter case, the integrals (4.8) are replaced by Riemann sums

ordinary differential equations given by (4.34) and (4.35) and then computing the expectations from (4.33) and the solution of (4.16). The crosses are based on the numerical solution of the system (4.3) and (4.4) and the expected values of the concentration defined by (4.8) are again replaced by a Riemann sum based on the numerical solution.

Table 4.1 Parameter values for the model of (4.1) and (4.2)

v_d	0.1 ms^{-1}
v_r	1.0 ms^{-1}
c_0	0 mM
c_1	1 mM
k_{co}	1 ms^{-1}
k_{oc}	1 ms^{-1}

4.3.5 Expected Concentrations in Equilibrium

In the case of constant rates, we derived the following system describing the evolution of the expected concentrations for open or closed channels, respectively,

$$e_o' = (v_r c_1 + v_d c_0)\,\pi_o + k_{co} e_c - (v_r + v_d + k_{oc})\,e_o, \tag{4.36}$$

$$e_c' = v_d c_0 \pi_c + k_{oc} e_o - (v_d + k_{co})\,e_c, \tag{4.37}$$

where we recall that

$$e_o = E_o \pi_o \text{ and } e_c = E_c \pi_c. \tag{4.38}$$

The stationary solution of this system is given as the solution of the following linear 2×2 system of equations:

$$\begin{pmatrix} k_{oc} + v_r + v_d & -k_{co} \\ -k_{oc} & k_{co} + v_d \end{pmatrix} \begin{pmatrix} e_o \\ e_c \end{pmatrix} = \begin{pmatrix} (v_r c_1 + v_d c_0)\,\pi_o \\ v_d c_0 \pi_c \end{pmatrix}, \tag{4.39}$$

where π_o and π_c are equilibrium probabilities given by (4.14) and (4.15). The solution of this system in terms of a formula becomes messy, but if we consider the specific parameters used in the computations (see Table 4.1), we find that the equilibrium expectations are given by

$$E_o = 0.8397 \text{ mM}, \tag{4.40}$$

$$E_c = 0.7634 \text{ mM}, \tag{4.41}$$

which compares well with our observations in Fig. 4.2.

4.4 Markov Model of a Mutation

Mutations may change the release mechanism and thus seriously alter the function of the calcium-induced calcium release. Mutations in the RyR2 gene can lead to changes in the receptor function, increasing the open probability.

Table 4.2 Parameter values for the model (4.43) and (4.44)

v_d	1 ms^{-1}
v_r	0.1 ms^{-1}
c_0	0.1 μM
c_1	1,000 μM
k_{co}	0.1 $\text{ms}^{-1}\mu\text{M}^{-1}$
k_{oc}	1 ms^{-1}

As mentioned above, one way to model the increased open probability is to define

$$k_{co,\mu} = \mu k_{co}, \tag{4.42}$$

where μ is referred to as the mutation severity index. This is a CO-mutation (see page 16) and it does not affect the mean open time. The parameter $\mu = 1$ denotes the wild type case and larger values of μ indicate more severe mutations. Basically, since $k_{co,\mu} > k_{co}$ for $\mu > 1$, the mutation will lead to an increased probability of being in the open state.

The system governing the open and closed probability densities now takes the form

$$\frac{\partial \rho_o}{\partial t} + \frac{\partial}{\partial x}(a_o \rho_o) = \mu k_{co}\, x \rho_c - k_{oc} \rho_o, \tag{4.43}$$

$$\frac{\partial \rho_c}{\partial t} + \frac{\partial}{\partial x}(a_c \rho_c) = k_{oc} \rho_o - \mu k_{co}\, x \rho_c, \tag{4.44}$$

where, as above, we have

$$\begin{aligned} a_o &= v_r(c_1 - x) + v_d(c_0 - x), \\ a_c &= v_d(c_0 - x). \end{aligned} \tag{4.45}$$

Note that in this model the opening rate depends on the concentration x. Model parameters are given in Table 4.2.

In Fig. 4.3, we show the results of Monte Carlo simulations (histograms) and solutions of the probability density system (4.43) and (4.44) (red solid line) for the wild type case ($\mu = 1$) and mutant case ($\mu = 3$). As above, we see that these two computational approaches give more or less the same answer. It is more interesting to observe the effect of the mutation. We see that the mutation tends to shift the open probability density function toward the upper boundary, where the function becomes very large. This shows that, in the case of mutation, it is very likely to have a high concentration *and* an open channel—much more likely than in the wild type case.

The statistical characteristics introduced above are given in Table 4.3. We note that the total open probability π_o increases from 0.811 for the wild type to 0.962 for the mutant. Also, we note that the expected concentration, E_o, for open channels is

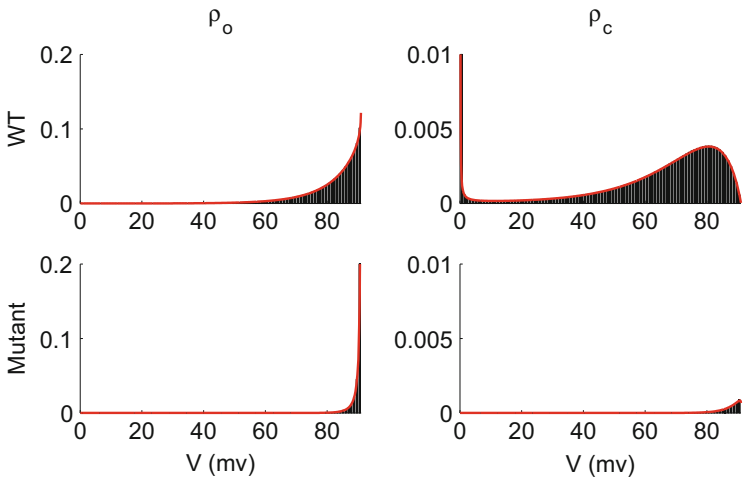

Fig. 4.3 *Upper panel*: Wild type open (*left*) and closed (*right*) probability density functions computed using Monte Carlo simulations (histogram) and by solving the probability density system (*red line*). The integral of the open probability density function is 0.811 (0.189 for the closed state probability density function). *Lower panel*: Similar figure as for the mutant case ($\mu = 3$). The integral of the open probability density function is 0.962 (0.038 for the closed state probability density function)

Table 4.3 Statistical properties of the wild type and mutant cases

Case	π_o	E_o	σ_o	π_c	E_c	σ_c
Wild type	0.811	81.91	9.50	0.189	43.04	35.26
Mutant	0.962	87.95	3.20	0.038	84.34	4.85

given by 81.91 μM for the wild type and 87.95 μM for the mutant. The standard deviation, on the other hand, is significantly reduced (by a factor of three) in the mutant case compared to the wild type. The probability of being in the closed state decreases by a factor of five in the mutant case compared to the wild type, whereas the expected concentration is doubled and the standard deviation is reduced by a factor of seven.

4.4.1 How Does the Mutation Severity Index Influence the Probability Density Function of the Open State?

We have seen a few examples indicating how changes in the reaction rates k_{co} and k_{oc} change the probability density functions. Since we are able to solve the stationary case analytically, this issue can be studied in great detail. Let us start by recalling that we model the effect of the mutation by introducing a severity index μ. The

stationary model is then

$$\frac{\partial}{\partial x}(a_o\rho_o) = \mu k_{co}\, x\rho_c - k_{oc}\rho_o, \tag{4.46}$$

$$\frac{\partial}{\partial x}(a_c\rho_c) = k_{oc}\rho_o - \mu k_{co}\, x\rho_c, \tag{4.47}$$

where we recall that $\mu = 1$ is the wild type case. We discussed above how to solve the steady state model analytically (see Sect. 2.6, page 41) and we can use the analytical solution to investigate how the mutation affects the probability density functions. Since the steady state open probability density function is given by the solution of

$$\rho_o' = -\alpha(x)\rho_o$$

with

$$\alpha(x) = \frac{\mu k_{co}\, x}{v_d(c_0 - x)} - \frac{v_p - k_{oc}}{v_p(c_+ - x)},$$

where

$$v_p = v_r \frac{c_1 - c_0}{c_+ - c_0},$$

we have solutions of the form

$$\rho_{o,\mu}(x) = K_\mu e^{\frac{\mu k_{co}\, x}{v_d}}(c_+ - x)^{\frac{k_{oc}}{v_p}-1}(x - c_0)^{\frac{c_0\mu k_{co}}{v_d}}, \tag{4.48}$$

where K_μ is a constant given by the somewhat complicated expression

$$1/K_\mu = (c_+ - c_0)^{a+b}e^a\Gamma(a)\Gamma(b)({}_1F_1(a, a+b, c) + k_{oc}\frac{v_p - v_d}{v_d v_p}{}_1F_1(a, a+b+1, c)).$$

Here ${}_1F_1$ is Kummer's regularized hypergeometric function and

$$a = c_0\mu k_{co}/v_d, b = k_{oc}/v_p, c = (c_+ - c_0)\mu k_{co}/v_d.$$

It is useful to consider the ratio of the mutant solution to the wild type solution and we find that

$$\frac{\rho_{o,\mu}(x)}{\rho_{o,1}(x)} = \frac{K_\mu}{K_1}e^{\frac{(\mu-1)xk_{co}}{v_d}}(x - c_0)^{\frac{(\mu-1)c_0k_{co}}{v_d}}.$$

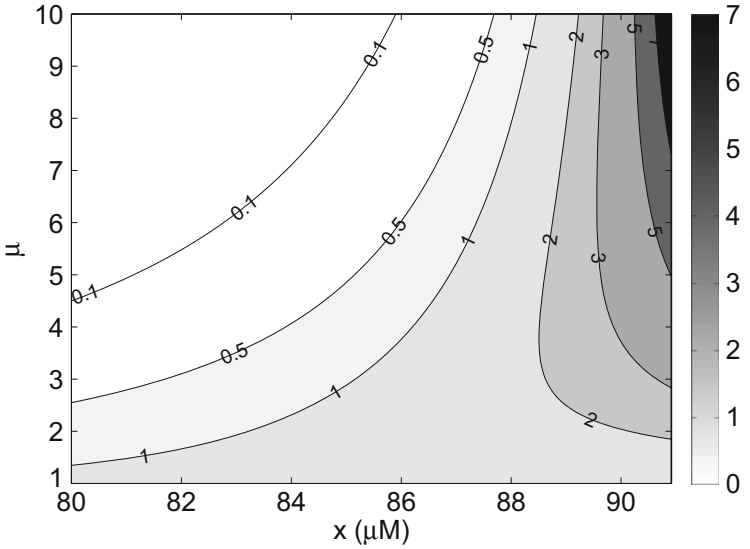

Fig. 4.4 Contours of the function $\frac{\rho_{o,\mu}(x)}{\rho_{o,1}(x)}$. Note that the open probability density function of the mutant is much greater than the open probability density function of the wild type for large values of the concentration and for large values of the mutation severity index μ

In Fig. 4.4, we graph this relation as a function of the severity index μ and the concentration x. We observe that, close to the maximum concentration, the open probability density function of the mutant is much larger than for the wild type.

4.4.2 Boundary Layers

As seen in both the numerical and analytical solutions above, the probability density functions may have singularities at the endpoints. It is easily seen from (4.48) that $\rho_{o,\mu}$ has a singularity at the endpoint $x = c_+$ whenever

$$\frac{k_{oc}}{v_p} < 1.$$

Similarly, we find that the closed probability density function is given by

$$\rho_{c,\mu}(x) = K_\mu \frac{v_p}{v_d} e^{\frac{\mu x k_{co}}{v_d}} (c_+ - x)^{\frac{k_{oc}}{v_p}} (x - c_0)^{\frac{\mu c_0 k_{co}}{v_d} - 1},$$

which has a singularity at $x = c_0$ whenever

$$\frac{\mu c_0 k_{co}}{v_d} < 1.$$

4.5 Statistical Properties as Functions of the Mutation Severity Index

We have seen, using numerical computations and analytical considerations, how the mutation severity index changes the probability density functions. In this section, we shall look with more detail into how the index changes the statistical properties of the probability density functions. Again, we consider a case where the rates k_{oc} and k_{co} are constants.

4.5.1 Probabilities

We recall that the open probability, defined as

$$\pi_o = \int_\Omega \rho_o dx, \tag{4.49}$$

evolves as

$$\pi_o(t) = \frac{k_{co}}{k_{co} + k_{oc}} \left(1 - e^{-(k_{co}+k_{oc})t}\right) \tag{4.50}$$

for wild type parameters in the case of $\pi_o(0) = 0$. If we introduce the mutation severity index in the Markov model (see (4.42)), we find that the open probability evolves as

$$\pi_{o,\mu}(t) = \frac{\mu k_{co}}{\mu k_{co} + k_{oc}} \left(1 - e^{-(\mu k_{co}+k_{oc})t}\right) \tag{4.51}$$

and thus the mutant case shows faster convergence toward a higher probability than the wild type case. In Fig. 4.5, we show the graphs of π_o and $\pi_{o,\mu}$ in the case of $\mu = 3$ and $\mu = 10$; the other parameters are given in Table 4.4.

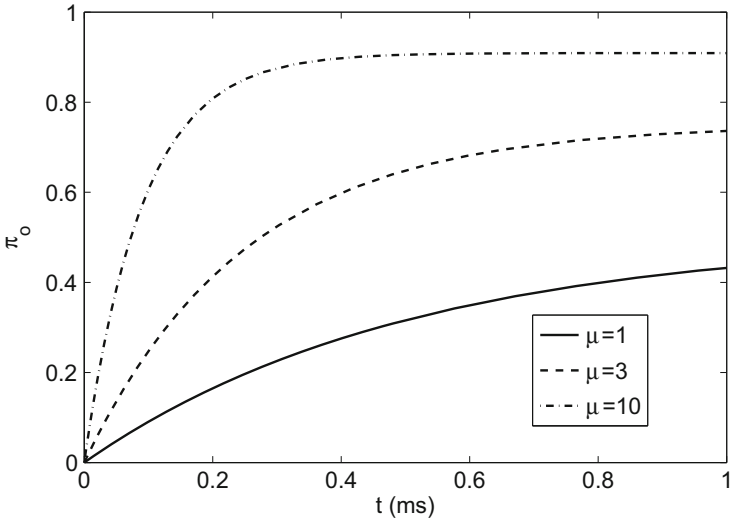

Fig. 4.5 The open probability π_o defined by (4.49) with $\mu = 1$ (wild type), $\mu = 3$, and $\mu = 10$. The mutation increases the equilibrium open probability and reduces the time to reach equilibrium

Table 4.4 Parameter values for the model (4.1) and (4.2) (copied from Table 4.1)

v_d	0.1 ms^{-1}
v_r	1.0 ms^{-1}
c_0	0 mM
c_1	1 mM
k_{co}	1 ms^{-1}
k_{oc}	1 ms^{-1}

4.5.2 Expected Calcium Concentrations

We defined the expected calcium concentrations in the case of open and closed channels as

$$E_o = \frac{1}{\pi_o}\int_\Omega x\rho_o dx \text{ and } E_c = \frac{1}{\pi_c}\int_\Omega x\rho_c dx. \tag{4.52}$$

Recall that π_o and π_c, are given by explicit formulas and that we introduced

$$e_o = E_o\pi_o \text{ and } e_c = E_c\pi_c. \tag{4.53}$$

For constant rates k_{oc} and k_{co}, the expectations can be found by solving the system of ordinary differential equations

$$e_o' = (v_r c_1 + v_d c_0)\,\pi_o + k_{co} e_c - (v_r + v_d + k_{oc})\,e_o, \tag{4.54}$$

$$e_c' = v_d c_0 \pi_c + k_{oc} e_o - (v_d + k_{co})\,e_c, \tag{4.55}$$

and then computing

$$E_o(t) = \frac{e_o(t)}{\pi_o(t)} \text{ and } E_c(t) = \frac{e_c(t)}{\pi_c(t)}.$$

In Fig. 4.6, we show the expected values of the calcium concentration for wild type data when the channel is open (solid, red) and closed (solid, blue), as well as mutant-type data ($\mu = 3$) when the channel is open (dotted, red) and closed (dotted, blue). In the computation using mutant data, we simply replace k_{co} with μk_{co}. However, keep in mind that this affects the formulas defining the probabilities π_o and π_c as well.

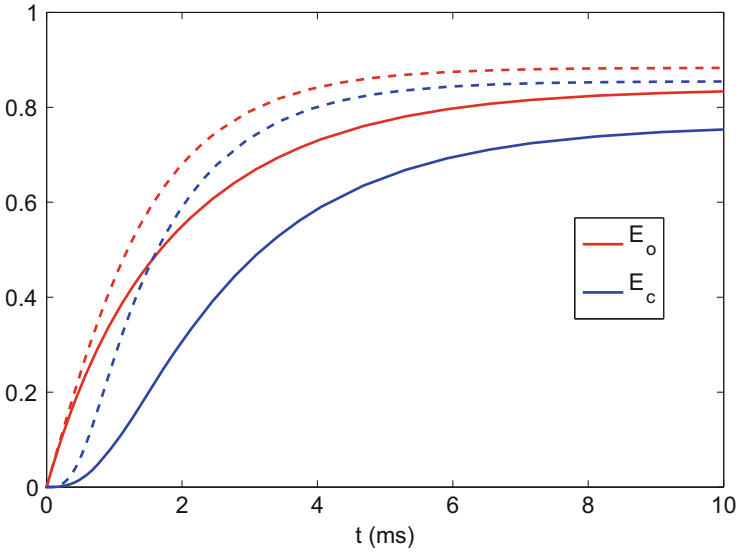

Fig. 4.6 Expected values of the concentration for wild type (*dotted lines*) and mutant (*solid lines*) cases as a function of time. In the mutant case, we used $\mu = 3$

4.5.3 Expected Calcium Concentrations in Equilibrium

As explained above, the equilibrium version of the expected concentrations E_o and E_c can be found by solving the following 2×2 linear system of equations:

$$\begin{pmatrix} k_{oc} + v_r + v_d & -\mu k_{co} \\ -k_{oc} & \mu k_{co} + v_d \end{pmatrix} \begin{pmatrix} e_o \\ e_c \end{pmatrix} = \begin{pmatrix} (v_r c_1 + v_d c_0)\, \pi_o \\ v_d c_0 \pi_c \end{pmatrix} \tag{4.56}$$

and then computing

$$E_o = \frac{e_o}{\pi_o} \text{ and } E_c = \frac{e_c}{\pi_c},$$

where π_o and π_c are equilibrium probabilities given by (4.14) and (4.15),

$$\pi_o = \frac{\mu k_{co}}{k_{oc} + \mu k_{co}}, \tag{4.57}$$

$$\pi_c = \frac{k_{oc}}{k_{oc} + \mu k_{co}}. \tag{4.58}$$

In Fig. 4.7, we plot the expectations as a function of the mutation severity index. The red line represents the expected value of the calcium concentration when the channel is open and the blue line represents the expected value of the calcium concentration

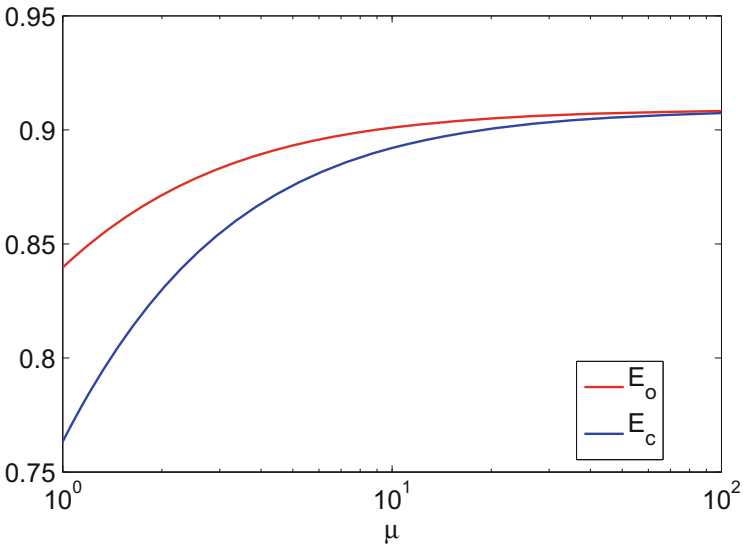

Fig. 4.7 Steady state of E_o and E_c as a function of the mutation severity index

when the channel is closed. Here, we use the parameters given in Table 4.4. The graphs start at $\mu = 1$, which represents the wild type case.

4.5.4 What Happens as $\mu \longrightarrow \infty$?

When the mutation severity index goes to infinity, we force the channel to be open more or less all the time. If we consider the stochastic model

$$\bar{x}'(t) = \bar{\gamma}(t)v_r(c_1 - \bar{x}) + v_d(c_0 - \bar{x})$$

as $\mu \longrightarrow \infty$, we know that the channel is generally open, so we have $\bar{\gamma}(t) \approx 1$. Therefore, we obtain the model

$$\bar{x}'(t) \approx v_r(c_1 - \bar{x}) + v_d(c_0 - \bar{x}).$$

As we have seen earlier, the equilibrium version of this equation is given by

$$x = c_+ = \frac{v_r c_1 + v_d c_0}{v_r + v_d} \approx 0.91 \text{ mM}$$

and this is what we see from the graphs of Fig. 4.7.

We can also see this from system (4.56). For the parameters given in Table 4.4, we have

$$\pi_o = \frac{\mu}{1+\mu} \text{ and } \pi_c = \frac{1}{1+\mu}$$

and therefore the system (4.56) takes the form

$$\begin{pmatrix} 2.1 & -\mu \\ -1 & \mu + 0.1 \end{pmatrix} \begin{pmatrix} e_o \\ e_c \end{pmatrix} = \begin{pmatrix} \frac{\mu}{1+\mu} \\ 0 \end{pmatrix}, \tag{4.59}$$

which, in terms of E_o and E_c, reads

$$\begin{pmatrix} 2.1 & -\mu\frac{\pi_c}{\pi_o} \\ -\pi_o & (\mu + 0.1)\pi_c \end{pmatrix} \begin{pmatrix} E_o \\ E_c \end{pmatrix} = \begin{pmatrix} 1 \\ 0 \end{pmatrix}. \tag{4.60}$$

If we let $\mu \longrightarrow \infty$, we obtain the system

$$\begin{pmatrix} 2.1 & -1 \\ -1 & 1 \end{pmatrix} \begin{pmatrix} E_o \\ E_c \end{pmatrix} = \begin{pmatrix} 1 \\ 0 \end{pmatrix} \tag{4.61}$$

and the solution

$$E_o = E_c \approx 0.91 \text{ mM}.$$

4.6 Statistical Properties of Open and Closed State Blockers

We have seen above that open and closed state theoretical blockers can significantly reduce the effect of the mutation. Computations have shown that closed state blockers repair the effect of the mutation as the parameter k_{bc} goes to infinity. This effect is also shown by a direct mathematical argument. For the open state blocker, we have seen that fairly good results can be obtained when the parameters of the drug are optimized, but perfect results can probably not be obtained for a CO-mutation because of the change of the mean open time described above. In this section, we present the statistical properties of the two types of drugs. The properties are presented in Table 4.5. In the table we observe that the total open probability (see Sect. 4.2, page 72) of the open state in the wild type case is 0.811. This increases to 0.962 for the mutant case ($\mu = 3$). When the closed state blocker is applied and the factor k_{bc} is increased, we see that the open probability is repaired by the drug. The same effect holds for the expected concentration E_o of the open state; it is completely repaired by the closed state blocker for large values of k_{bc}. This also holds for the standard deviation. For the open state blocker, we do not obtain a sufficient effect by increasing k_{bo}, but when both parameters of the drug are optimized, the open probability and the expected concentration of the open state are almost completely repaired. The open state blocker is, however, unable to repair the standard deviation.

Table 4.5 Statistical properties of the closed and open state blockers

Case	π_o	E_o	σ_o
Closed blocker, k_{bc}=10	0.739	82.47	10.59
Closed blocker, k_{bc}=100	0.805	81.97	9.66
Closed blocker, k_{bc}=1,000	0.811	81.91	9.52
Open blocker, k_{bo}=1	0.935	86.85	6.45
Open blocker, k_{bo}=10	0.936	85.97	4.89
Open blocker, k_{bo}=100	0.936	85.80	3.44
Optimized open blocker	0.817	80.09	13.10
Wild type, no drug	0.811	81.91	9.50
Mutant, no drug	0.962	87.95	3.20

4.7 Stochastic Simulations Using Optimal Drugs

We derived closed state and open state blockers with the parameters summarized in Table 3.2. In Fig. 4.8, we show the solutions of the stochastic model

$$\bar{x}'(t) = \bar{\gamma}(t)v_r(c_1 - \bar{x}) + v_d(c_0 - \bar{x}) \tag{4.62}$$

computed using the scheme

$$x_{n+1} = x_n + \Delta t\left(\gamma_n v_r(c_1 - x_n) + v_d(c_0 - x_n)\right), \tag{4.63}$$

where the dynamics of the stochastic function γ are given by the Markov model. The wild type solution is given in the upper-left part of the solution and we observe significantly larger variations than for the solution in the mutant case (upper right). The effect of the mutation is well repaired by both drugs. Note that since a random number is used in every time step, the solutions will never coincide, no matter how good the drug is. This illustrates the difficulty of comparing stochastic solutions and shows that comparison using probability density functions and derived statistics is much easier.

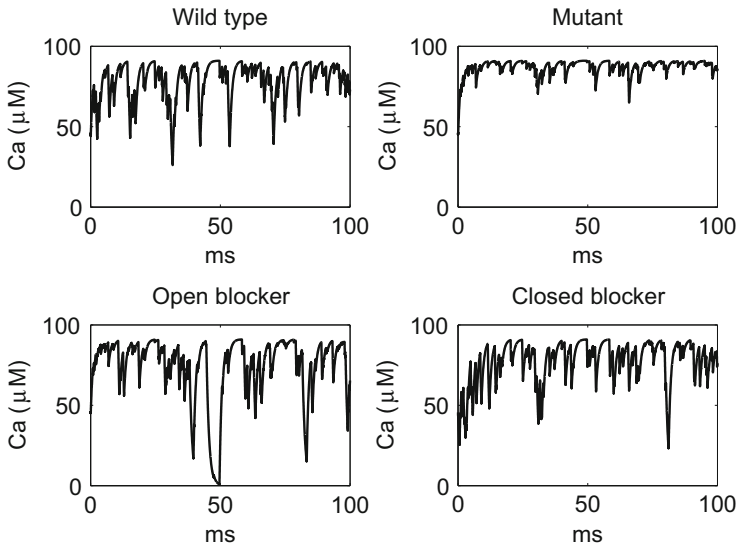

Fig. 4.8 Simulations based on the stochastic model (4.62) computed using scheme (4.63). In the mutant case, we use $\mu = 3$. The parameters specifying the drugs are given in Table 3.2

4.8 Notes

1. The mean open time will be introduced and analyzed in Chap. 13. In the present chapter, we have just used the very basic properties.
2. The statistical properties discussed in this chapter are taken from Williams et al. [103].